IEEE Access
Multidisciplinary | Rapid Review | Open Access Journal

Received April 20, 2019, accepted May 18, 2019, date of publication May 22, 2019, date of current version June 6, 2019.

Digital Object Identifier 10.1109/ACCESS.2019.2918194

Adaptive Packet-Length Assisted Random Access Scheme in LEO Satellite Network

JIALING BAI AND GUANGLIANG REN, (Member, IEEE)
State Key Laboratory of Integrated Service Networks, Xidian University, Xi'an 710071, China

Corresponding author: Guangliang Ren (glren@mail.xidian.edu.cn)

This work was supported in part by the National Natural Science Foundation of China under Grant 91538105, and in part by the National Natural Science Foundation of China under Grant 61801352.

ABSTRACT A new adaptive packet-length assisted random access (RA) scheme is proposed to improve the performance of the RA system in LEO satellite network. In the scheme, the lengths of data packets are adaptively selected with different modulation and coding schemes (MCSs) according to the transmission quality of the LEO satellite link. Based on the adaptive packet length, the protocols based on advanced slotted ALOHA are modified and analyzed. The simulation results show that the throughput of the adaptive packet-length assisted CRDSA (APL-CRDSA) is about 1.5 times larger than that of the conventional CRDSA. The packet loss rate (PLR) performance and the energy efficiency performance of the APL-CRDSA are also greater than those of the conventional CRDSA.

INDEX TERMS Adaptive packet length, different modulation and coding schemes (MCSs), advanced slotted ALOHA.

I. INTRODUCTION

LOW-earth-orbit (LEO) satellite network is one of the most important networks in the internet of thing (IoT) oriented satellite networks. Due to the low propagation delay and the low propagation attenuation, LEO satellite network allows low-power machine type communication (MTC) terminals to access the network. Among the available access techniques, random access (RA) is considered as the most suitable technique for the traffic of MTC terminals. However, the available RA protocols cannot meet the requirement of the massive number of MTC terminals to access the network due to their low throughputs.

To satisfy the requirement, some new high-throughput RA schemes have attracted much more attentions in recent years. Since 2007, several RA schemes, such as contention resolution diversity Slotted ALOHA (CRDSA) [1], CRDSA++ [2] and irregular repetition Slotted ALOHA (IRSA) [3], [4], have been proposed. The key idea of these schemes is to send regular or irregular replicas of the same packet with equal power at the transmitter side, and to exploit successive interference cancellation (SIC) technique to resolve collisions at the receiver side. Coded Slotted ALOHA (CSA) protocol [5] has been introduced later. In CSA, each data packet is divided into several segments and these segments are encoded instead of simply repeated in CRDSA and IRSA. In these advanced schemes, the maximum normalized throughput is about 0.8. To further improve the throughput, the polarized MIMO Slotted ALOHA (PMSA) [6] is employed to resolve collisions in the SA scheme, in which the maximum normalized throughput is about 0.84. In all the available RA schemes, it is found that the length and the other parameters of data packets are fixed since the worst transmission quality of the link is considered to choose the parameters of packets. Transmission losses from MTC terminals to satellite nodes are different within the coverage area of LEO satellite, due to the different distances. Thus the transmission qualities of MTC terminals in the uplink are different. In all the available RA protocols, the quality difference in the uplink is ignored, but it is important information to adjust the parameters of packets. The packets with different parameters for a given transmission quality may provide an additional degree of freedom for RA to improve its throughput.

To further improve the throughput of RA scheme, we propose an adaptive packet-length (APL) assisted RA scheme for the type of advanced CRDSA protocols, by making full use of the information of the transmission quality. In the proposed scheme, the packet length can be adaptively changed according to the transmission quality with different modulation and coding schemes (MCSs), and the protocol is modified to adapt to the packets with different lengths. The proposed scheme outperforms the conventional RA schemes

The associate editor coordinating the review of this manuscript and approving it for publication was Zhong Fan.

in throughput, packet loss rate (PLR) and energy efficiency. In addition, the idea of APL assisted can also be applied into other SA class protocols to further improve their throughput performance.

The rest of this paper is organized as follows. In Section II, system model is given. The APL-assisted scheme and throughput analysis are proposed in Section III. In Section IV, simulation results are discussed. Finally, in Section V, the conclusions are given.

II. SYSTEM MODEL

The simple IoT oriented LEO satellite network consists of several LEO satellite nodes, some MTC base stations (MBSs) and a gateway station, and its configuration is shown in Fig.1. There are a large number of MBSs distributed in a large coverage area accessing the satellite nodes through a shared RA channel. Each MBS collects data from active MTC terminals in its coverage area and packs the message into packets. The LEO satellite node receives packet signals from MBSs and sends the received data to the gateway station through the satellite network. The gateway station processes and decodes the received data and broadcasts the control information to MBSs through the satellite network.

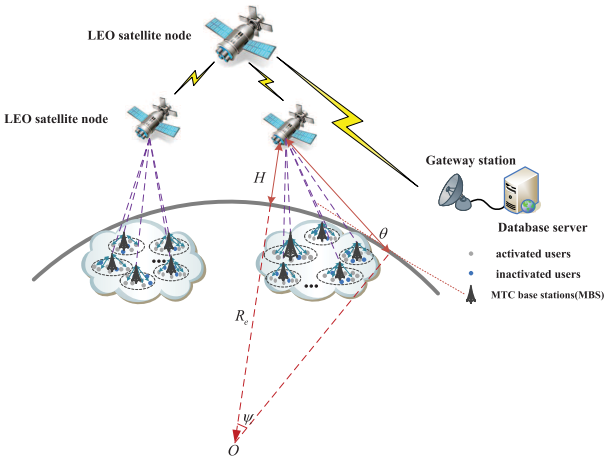

FIGURE 1. Configuration of LEO satellite network.

A. TRANSMISSION QUALITIES OF THE UPLINKS

Generally, LEO satellite is in circular orbits at altitudes ranging from 500 km to 2000 km. The real-time coverage area of satellite depends on the satellite altitude H and the minimum elevation angle θ required for the MBSs located at the edge of the coverage area [7]. The coverage area changes as the movement of LEO satellite node.

In LEO satellite system, the distance to satellite can be measured according to the position information of the MBS and the location of the satellite node in its trajectory. The distance is time varying due to the movement of the satellite node. The distance L from the MBS to the satellite node can be expressed as Eq.(1).

$$L = \sqrt{(R_e + H)^2 + {R_e}^2 - 2(R_e + H)R_e \cos\psi} \tag{1}$$

where R_e expresses the average radius of the earth, ψ is the angular coverage and $\psi = \cos^{-1}\left(\frac{R_e \cos\theta}{R_e+H}\right) - \theta$. θ is the elevation angle from the MBS to the satellite node. According to the satellite link budget in [8], the received SNR, as one of the metrics of transmission quality in the uplink, is closely related to the propagation loss that is caused by the distance L. Therefore, the received SNRs from different MBSs will be different and the difference in the SNRs gives an additional degree of freedom for MBSs to adjust the parameters of their packets to improve the performance of the RA scheme.

B. TRANSMISSION MODEL

In the IoT oriented LEO satellite uplink, the single-carrier interleave frequency division multiple access (SC-IFDMA) signal is often employed in physical layer to carry data for its constant envelope characteristics with the low order modulation, as in [9], [10]. With the SC-IFDMA signal, the MBSs send data in the form of packet and the structure of data packets refers to that in the return link of DVB-RCS2 system [11]. Each packet contains preamble symbols, payload symbols and post-amble symbols, in addition, pilot symbols are uniformly inserted into data symbols. It is assumed that there are N bits in a packet for the u^{th} MBS. Then the N bits are encoded [12] by the encoder with the code rate $R^{(u)}$, and the encoded bits are modulated by the modulator with the order of $D^{(u)}$. The transmitted complex modulated data of the m^{th} SC-IFDMA symbol in the i^{th} slot can be represented as $\mathbf{x}_i^{(u)}(m)$, and then it is converted to the data in frequency domain by N_u-point discrete Fourier transform $\mathbf{F}_{N_u}$. The signals in frequency domain are mapped to N_u inputs of an N-point inverse FFT (IFFT) block with the interleaved subcarrier mapping mode. The mapped signal is given by $\mathbf{X}_i^{(u)}(m) = \mathbf{T}^{(u)}\mathbf{F}_{N_u}\mathbf{x}_i^{(u)}(m)$, where $\mathbf{T}^{(u)}$ is a subcarrier mapping matrix for the u^{th} MBS. Finally, N-point inverse FFT (IFFT), $\mathbf{F}_N^H$ is employed to $\mathbf{X}_i^{(u)}(m)$ and cyclic prefix (CP) is appended. Thus the transmitted SC-IFDMA signal can be written as Eq.(2).

$$\begin{aligned}\tilde{\mathbf{x}}_i^{(u)}(m) &= \mathbf{F}_N^H \mathbf{X}_i^{(u)}(m) \\ &= \mathbf{F}_N^H \mathbf{T}^{(u)} \mathbf{F}_{N_u} \mathbf{x}_i^{(u)}(m)\end{aligned} \tag{2}$$

where $u = 1, \ldots, U$, $m = 0, 1, \ldots, M' - 1$, U is the total number of MBSs, M' represents the number of SC-IFDMA symbols in a data packet.

To ensure the reliability of packet transmission in the worst condition, the modulation and coding scheme with the lowest order to carry N bits is employed for conventional RA schemes. The SC-IFDMA based packet is transmitted in one of slots in the conventional time division multiple access (TDMA) frame [1]–[3] with the duration of T_F. Each frame is composed of M_{slots}^{RA} slots, each slot carries one packet, and the duration of each slot is T_P, ($T_P = T_F/M_{slots}^{RA}$), as shown in Fig.2.

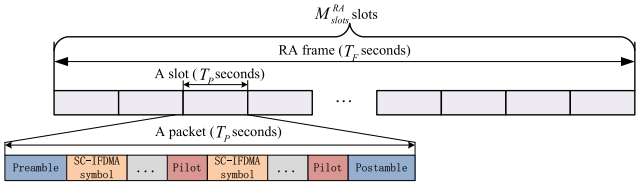

FIGURE 2. Structure of RA frame in satellite uplinks.

To ensure the reliability of packet transmission and adapt to different transmission conditions, different MCSs can be used to generate packets, and the number of SC-IFDMA symbols carrying the data will be different. That is, the packet length will be different.

III. PROPOSED RANDOM ACCESS SCHEME

In the proposed scheme, the MBS can select a suitable MCS to generate the packet according to its transmission quality. The duration of the packet may be much less than that of the slot in frame, thus most of the time may be idle in the slot, except the duration of the packet. To increase the number of access channels, we divided the slot into sub-sots to transmit packets with different lengths. The MBS transmits its packet in accordance with RA protocol into sub-slots, and the packets with different time durations (or lengths) in the received signals are jointly processed. In order to process the received signals at the gateway conveniently, the number of the sub-slots in one slot is often selected as an integral number in the frame. Specifically, we take the popular CRDSA protocol as an example to describe the proposed scheme and the detail of the APL-assisted CRDSA (APL-CRDSA) is given as follows.

A. GENERATION OF THE DATA PACKET WITH ADAPTIVE PACKET-LENGTH

The MBSs can estimate SNRs in their uplinks by computing the propagation loss with their positions and two-line orbital elements (TLE) of LEO satellites, or by measuring the received power of broadcasting signal in the downlink. Based on the estimated SNRs, the MBS can choose a suitable MCS to generate data packet with a given packet length by using the mapping table of SNRs and MCSs. The mapping table is constructed for a given packet error rate (PER) in advance.

In general, we assume that there are M different MCSs and their corresponding received SNR ranges in the mapping table for the given payload, and the M different packet lengths $P_1, P_2, \ldots, P_M$ corresponds to the M MCSs. The durations of packets corresponding to the M different lengths can be expressed as $T_{P1}, T_{P2}, \ldots, T_{PM}, (T_{P1} > T_{P2} > \ldots > T_{PM})$ respectively. In the proposed schemes, the number of packets carried by a slot is different, which is related to the length of packets with its selected MCS. Assuming that the duration of packet with a length of P_i is T_{Pi}, $(i = 1, \ldots, M)$, then the maximum number of packets with a length of P_i that can be carried by each time slot is T_P/T_{Pi}, $(i = 1, \ldots, M)$. Particularly, when $i = 1$, there is $T_{P1} = T_P$, that is, each slot can carry a packet with a duration of T_{P1}. As mentioned above, each frame consists of M_{slots}^{RA} slots, thus the maximum number of packets with a length of T_{Pi} that each frame can carry is T_F/T_{Pi}, for $i = 1, \ldots, M$. A more intuitive description of the distribution of packets with different lengths without collisions can be shown in Fig.3.

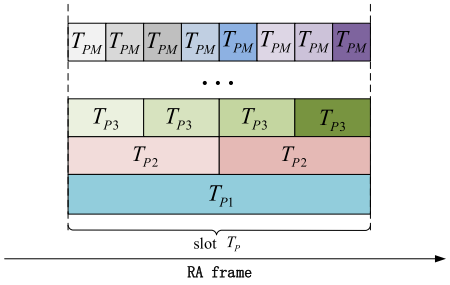

FIGURE 3. Diagram of data packets with different lengths.

To distinguish these packets with different lengths conveniently, M preamble sets $S_1, S_2, \ldots, S_M$ are employed for the M different packet lengths. Each MBS randomly selects a preamble from the sets corresponding to its length in the generation of the packet.

B. APL-CRDSA SCHEME

In APL-CRDSA, the received SNR, as the metric of transmission quality parameter, is firstly estimated by the computation of the propagation loss at MBSs. Then with the estimated SNR, a suitable MCS is selected to generate SC-IFDMA symbols to carry the N bits information. The packet length is determined by the number of the SC-IFDMA symbols. The preamble is selected from the preamble set corresponding to the packet length. Pilots, post-ambles and information symbols are combined to generate the data packet. The RA frame with the fixed duration of T_F is divided into T_F/T_{Pi} sub-slots for the packet with the length of P_i, $(i = 1, \ldots, M)$. Afterwards, the MBS randomly selects two sub-slots to transmit its twins of the same packets according to the CRDSA protocol.

It is noted that the shorter duration of a packet will bring more sub-slots in the frame, which will bring a greater throughput for RA scheme. So it is desired that the MBS can transmit its information with short packet as possible. To make packets aligned in the slot, the longest packet is selected as an integral multiple of other packet lengths.

At the receiver side in the satellite nodes, the received signal in slots may contain packets with different lengths, which is different from that in the conventional CRDSA scheme. The idea of the received signal processing in APL-CRDSA is the same as that in the conventional CRDSA, but the decoding of clean packets and the SIC process will be more complicated. At the first iteration in APL-CRDSA, the preambles of packets are searched and detected in each sub-slot in parallel in the duration of the TDMA frame at the gateway station.

The positions of data packets are recorded in the memory for the subsequent iterative decoding process conveniently. According to the recorded position information, if the data packet with the length of P_i has not been interfered by other bursts within its duration of T_{Pi}, $(i = 1, \ldots, M)$, it is regarded as clean. Then the clean packet is decoded and its interference to other packets is reconstructed and cancelled from the received signals. Following the above processing, the remained signal will be iteratively processed within the maximum number of iterations, as in CRDSA. The detailed algorithm steps are presented in **Algorithm 1**.

Algorithm 1 Proposed APL-CRDSA Based on the SIC Technique

1: Initialization: set the maximum number of iterations and the current number of iteration to $N_{iter}^{\max}$ and $N_{iter} = 1$, respectively.
2: Determine and record the positions of data packets with different lengths in each sub-slot of the frame by the search and detection of all the possible preambles from the preamble sets of $S_1, S_2, \ldots, S_M$ for the subsequent decoding process.
3: Search and decode the clean packet with the duration of T_{Pi}, $(i = 1, \ldots, M)$ with the recorded positions of data packets.
4: Reconstruct the replica from packet with the decoded bits based on the step3 in the form of SC-IFDMA, and cancel its interference from the collided packets as that in CRDSA.
5: Increase the iteration counter as: $N_{iter} = N_{iter} + 1$.
6: If the iteration number does not exceed maximum iteration number $N_{iter}^{\max}$, go to step 2; else stop.

The detailed decoding process is illustrated with an example in Fig.4. In this example, a frame with 8 slots and 10 MBSs is considered. Three different packet lengths of P_1, P_2 and P_3 are assumed here, which have the corresponding durations of T_{P1}, T_{P2} and T_{P3} respectively.

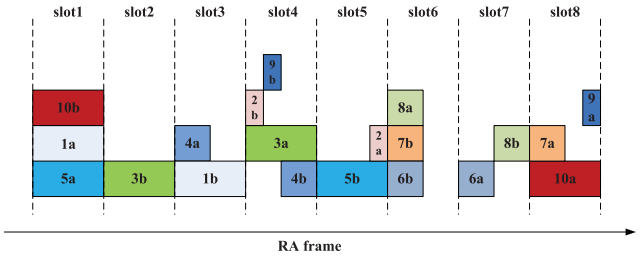

FIGURE 4. Example of the received frame in the APL-CRDSA scheme.

Firstly, according to the step 3, clean packet 3b in slot2 can be decoded successfully, then its information can be used to cancel the interference caused by 3a in slot4. Since the packets in slot4 are not overlapped after packet 3a is removed, packet 2b in slot4 can be decoded successfully when searching the matched preamble, and its interference in slot5 can be cancelled. The packet 9 and packet 4 have the same decoding process as packet 2. Next, packets 5b in slot5 will be recovered by removing the interference generated by packet 2a. After packets 6a and 8b in slot7 are decoded consecutively, clean packets are all recovered at the first iteration. At the second iteration process, packets 1, 7 and 10 will be recovered one after another. Therefore, all the collided packets can be decoded with APL-assisted. The order in which packets are successfully decoded is shown as follows.

$$3 \rightarrow 2 \rightarrow 9 \rightarrow 4 \rightarrow 5 \rightarrow 6 \rightarrow 8 \rightarrow 1 \rightarrow 7 \rightarrow 10 \quad (3)$$

However, only packet 3 can be recovered successfully for the conventional CRDSA protocol with SIC. All the others will be lost, due to the packets collisions.

The APL-assisted CRDSA-3 (APL-CRDSA-3) and the APL-assisted IRSA (APL-IRSA) have the similar generation process of packets as in APL-CRDSA. The difference among them lies in the number of replicas. At the gateway station, the search and SIC process will become more complicated as the number of replicas increases. For simplicity, the description of APL-CRDSA-3 and APL-IRSA will not be repeated here.

C. THROUGHPUT ANALYSIS OF APL-ASSISTED SCHEMES

In this section, the upper and lower bounds for the throughput of APL-CRDSA scheme with M different packet lengths are derived. Referred to the derivation in CRDSA [1], it is assumed that the probability of preamble collision can be negligible. Thus the throughput $Thr(N_{iter}|G)$ and the probability of successfully decoding $P(N_{iter}|G)$ are the functions of the iteration number N_{iter} for a normalized load G, which can be expressed as Eq.(4).

$$Thr(N_{iter}|G) = G \cdot P(N_{iter}|G) \quad (4)$$

$$\begin{aligned} P(N_{iter}|G) &= 1 - \left[\left(1 - P^A(N_{iter}|G)\right) \cdot \left(1 - P^B(N_{iter}|G)\right)\right] \\ &= 1 - \left[\left(1 - P^A(N_{iter}|G)\right)^2\right] \end{aligned} \quad (5)$$

where $P^A(N_{iter}|G)$ and $P^B(N_{iter}|G)$ are the probability that replicas A and B of the same packet are successfully decoded at the iteration N_{iter} for a normalized load G, and $P^A(N_{iter}|G) = P^B(N_{iter}|G)$. The bound for the probability $P^A(N_{iter}|G)$ can be represented as follows.

$$P^A(N_{iter}|G) \leq P_{al}^A(G) + \sum_{i=1}^{G \cdot M_{slots}^{RA} - 1} P_{int}(i|G) \cdot [P^A(N_{iter} - 1|G)]^i \quad (6)$$

where $P_{al}^A(G)$ represents the probability that data packet is clean in the slot, and $P_{int}(i|G)$ represents the probability that the useful packet is colliding with i interfering packets on the same slot. $G \cdot M_{slots}^{RA} - 1$ represents the maximum number of interfering packets that can be present in one slot, which is assumed to be an integer. The so called "loops" has not been considered, as in CRDSA [1].

The derivations of $P_{al}^{A}(G)$ and $P_{int}(i|G)$ are the same as in CRDSA and they can be expressed as follows.

$$P_{al}^{A}(G) = P_{int}(0|G) = [1 - P\{p_k \in S_n\}]^{G \cdot M_{slots}^{RA} - 1} \tag{7}$$

$$P_{int}(i|G) = \binom{G \cdot M_{slots}^{RA} - 1}{i} [P\{p_k \in S_n\}]^i \cdot [1 - P\{p_k \in S_n\}]^{G \cdot M_{slots}^{RA} - 1 - i} \tag{8}$$

where $P\{p_k \in S_n\}$ is the corresponding probability that the packet p_k presents on a given slot S_n. Taking Eq.(7) and Eq.(8) into Eq.(6), we can get Eq.(9), as shown at the bottom of this page.

In Eq.(9), the second part can be denoted as the function of Q, for the convenience of derivation, which is shown as Eq.(10), as shown at the bottom of this page.

Then Eq.(10) can be transformed as Eq.(11), as shown at the bottom of this page.

In Eq.(11), Q' can be regarded as the expansion of binomial, and we can show Eq.(12), as shown at the top of the next page.

Taking Eq.(12) into Eq.(11), thus we can get Eq.(13), as shown at the top of the next page.

Next, bringing Q back to original Eq.(9), it can be represented as Eq.(14), as shown at the top of the next page.

Finally, Eq.(9) can be rewritten as Eq.(15), as shown at the top of the next page. The initial value of $P^A(\cdot)$ is 0 in Eq.(15). It is noteworthy that $P\{p_k \in S_n\}$ determines the term $P^A(N_{iter}|G)$, and the smaller $P\{p_k \in S_n\}$ will lead to the bigger $P^A(N_{iter}|G)$. The derivation is shown as follows.

After the first iteration for Eq.(15), we can show that $P^A(1|G) \leq (1 - P\{p_k \in S_n\})^{G \cdot M_{slots}^{RA} - 1}$, $P\{p_k \in S_n\}$ and $P^A(1|G)$ have the opposite change trend. Thus the smaller $P\{p_k \in S_n\}$ will result in smaller $(1 - P^A(1|G))$ and bigger $1 - P\{p_k \in S_n\} \cdot (1 - P^A(1|G))$ in Eq.(15), besides, the bigger $P^A(2|G)$. Then the iteration process will continue until the maximum iteration number, we can get the above conclusion.

In APL-CRDSA, $P\{p_k \in S_n\}$ is closely related to the number of sub-slots T_F/T_{Pi} in a frame corresponding to the length P_i, $(i = 1, \ldots, M)$, which can be computed

$$\begin{aligned} P^A(N_{iter}|G) &\leq P_{al}^{A}(G) + \sum_{i=1}^{G \cdot M_{slots}^{RA} - 1} P_{int}(i|G) \cdot [P^A(N_{iter} - 1|G)]^i \\ &\leq [1 - P\{p_k \in S_n\}]^{G \cdot M_{slots}^{RA} - 1} \\ &\quad + \underbrace{\sum_{i=1}^{G \cdot M_{slots}^{RA} - 1} \binom{G \cdot M_{slots}^{RA} - 1}{i} [P\{p_k \in S_n\}]^i \cdot [1 - P\{p_k \in S_n\}]^{G \cdot M_{slots}^{RA} - 1 - i} \cdot [P^A(N_{iter} - 1|G)]^i}_{Q} \end{aligned} \tag{9}$$

$$\begin{aligned} Q &= \sum_{i=1}^{G \cdot M_{slots}^{RA} - 1} P_{int}(i|G) \cdot [P^A(N_{iter} - 1|G)]^i \\ &= \sum_{i=1}^{G \cdot M_{slots}^{RA} - 1} \binom{G \cdot M_{slots}^{RA} - 1}{i} [P\{p_k \in S_n\}]^i \cdot [1 - P\{p_k \in S_n\}]^{G \cdot M_{slots}^{RA} - 1 - i} \cdot [P^A(N_{iter} - 1|G)]^i \end{aligned} \tag{10}$$

$$\begin{aligned} Q &= \sum_{i=1}^{G \cdot M_{slots}^{RA} - 1} \binom{G \cdot M_{slots}^{RA} - 1}{i} [P\{p_k \in S_n\}]^i \cdot [1 - P\{p_k \in S_n\}]^{-i} \cdot [1 - P\{p_k \in S_n\}]^{G \cdot M_{slots}^{RA} - 1} \cdot [P^A(N_{iter} - 1|G)]^i \\ &= \sum_{i=1}^{G \cdot M_{slots}^{RA} - 1} \binom{G \cdot M_{slots}^{RA} - 1}{i} \left[\frac{P\{p_k \in S_n\}}{1 - P\{p_k \in S_n\}}\right]^i \cdot [P^A(N_{iter} - 1|G)]^i \cdot [1 - P\{p_k \in S_n\}]^{G \cdot M_{slots}^{RA} - 1} \\ &= \sum_{i=1}^{G \cdot M_{slots}^{RA} - 1} \binom{G \cdot M_{slots}^{RA} - 1}{i} \left[\frac{P\{p_k \in S_n\}}{1 - P\{p_k \in S_n\}} \cdot P^A(N_{iter} - 1|G)\right]^i \cdot [1 - P\{p_k \in S_n\}]^{G \cdot M_{slots}^{RA} - 1} \\ &= \underbrace{\sum_{i=1}^{G \cdot M_{slots}^{RA} - 1} \binom{G \cdot M_{slots}^{RA} - 1}{i} \left[\frac{P\{p_k \in S_n\}}{1 - P\{p_k \in S_n\}} \cdot P^A(N_{iter} - 1|G)\right]^i \cdot 1^{G \cdot M_{slots}^{RA} - 1 - i}}_{Q'} \cdot [1 - P\{p_k \in S_n\}]^{G \cdot M_{slots}^{RA} - 1} \end{aligned} \tag{11}$$

$$
\begin{aligned}
Q' &= \sum_{i=1}^{G\cdot M_{slots}^{RA}-1} \binom{G\cdot M_{slots}^{RA}-1}{i} \left[\frac{P\{p_k \in S_n\}}{1-P\{p_k \in S_n\}} \cdot P^A(N_{iter}-1|G)\right]^i \cdot 1^{G\cdot M_{slots}^{RA}-1-i} \\
&= \left(1+\frac{P\{p_k \in S_n\}\cdot P^A(N_{iter}-1|G)}{1-P\{p_k \in S_n\}}\right)^{G\cdot M_{slots}^{RA}-1} - \binom{G\cdot M_{slots}^{RA}-1}{0} \left[\frac{P\{p_k \in S_n\}}{1-P\{p_k \in S_n\}} \cdot P^A(N_{iter}-1|G)\right]^0 \cdot 1^{G\cdot M_{slots}^{RA}-1} \\
&= \left(1+\frac{P\{p_k \in S_n\}\cdot P^A(N_{iter}-1|G)}{1-P\{p_k \in S_n\}}\right)^{G\cdot M_{slots}^{RA}-1} - 1
\end{aligned} \tag{12}
$$

$$
\begin{aligned}
Q &= \left(\left(1+\frac{P\{p_k \in S_n\}\cdot P^A(N_{iter}-1|G)}{1-P\{p_k \in S_n\}}\right)^{G\cdot M_{slots}^{RA}-1} - 1\right)\cdot[1-P\{p_k \in S_n\}]^{G\cdot M_{slots}^{RA}-1} \\
&= \left(\left(1+\frac{P\{p_k \in S_n\}\cdot P^A(N_{iter}-1|G)}{1-P\{p_k \in S_n\}}\right)\cdot(1-P\{p_k \in S_n\})\right)^{G\cdot M_{slots}^{RA}-1} - [1-P\{p_k \in S_n\}]^{G\cdot M_{slots}^{RA}-1} \\
&= \left((1-P\{p_k \in S_n\}) + P\{p_k \in S_n\}\cdot P^A(N_{iter}-1|G)\right)^{G\cdot M_{slots}^{RA}-1} - [1-P\{p_k \in S_n\}]^{G\cdot M_{slots}^{RA}-1} \\
&= \left(1-P\{p_k \in S_n\}\cdot(1-P^A(N_{iter}-1|G))\right)^{G\cdot M_{slots}^{RA}-1} - [1-P\{p_k \in S_n\}]^{G\cdot M_{slots}^{RA}-1}
\end{aligned} \tag{13}
$$

$$
\begin{aligned}
P^A(N_{iter}|G) \le\ & [1-P\{p_k \in S_n\}]^{G\cdot M_{slots}^{RA}-1} \\
&+ \left(1-P\{p_k \in S_n\}\cdot(1-P^A(N_{iter}-1|G))\right)^{G\cdot M_{slots}^{RA}-1} - [1-P\{p_k \in S_n\}]^{G\cdot M_{slots}^{RA}-1}
\end{aligned} \tag{14}
$$

$$
P^A(N_{iter}|G) \le \left(1-P\{p_k \in S_n\}\cdot(1-P^A(N_{iter}-1|G))\right)^{G\cdot M_{slots}^{RA}-1} \tag{15}
$$

as Eq.(16).

$$
\begin{aligned}
P\{p_k \in S_n\} &= P\{p_k^A \in S_n\} + P\{p_k^A \notin S_n\} \\
&\cdot P\{p_k^B \in S_n\} = \frac{2}{T_F/T_{Pi}}
\end{aligned} \tag{16}
$$

From Eq.(16), we can observe that the probability $P\{p_k \in S_n\}$ is different for the packets with different lengths and the shorter duration of packets will lower this probability.

Let $P_{P_1}^A(N_{iter}|G)$ and $P_{P_M}^A(N_{iter}|G)$ express the probability of successfully decoding that all the MBSs only send the packets with the length of P_1 or the length of P_M respectively. Thus based on the derivation above, we can obtain that,

$$
P_{P_1}^A(N_{iter}|G) \le P^A(N_{iter}|G) \le P_{P_M}^A(N_{iter}|G) \tag{17}
$$

Substituting Eq.(17) into Eq.(5) and then taking Eq.(5) into Eq.(4) successively, the conclusion can be derived as follows.

$$
Thr_{P_1}(N_{iter}|G) \le Thr(N_{iter}|G) \le Thr_{P_M}(N_{iter}|G) \tag{18}
$$

where $Thr_{P_1}(N_{iter}|G)$ expresses the throughput function of all the MBSs sending the packets with the length of P_1. $Thr_{P_M}(N_{iter}|G)$ expresses the throughput function of all the MBSs sending the packets with the length of P_M.

IV. NUMERICAL RESULTS

The performance of APL-CRDSA, APL-CRDSA-3 and APL-IRSA with $\Lambda_3(x) = 0.5x^2 + 0.28x^3 + 0.22x^8$ is investigated and compared with their conventional ones by the computer simulation. In all the simulations, it is assumed that the satellite altitude H above the ground is about 780km, and the minimum elevation angle is set to 16°. The transmitted power is 100mW. The deployment of MBSs follows the uniform distribution within the coverage area of LEO satellite. The effects of channel fading and noise are considered in simulations. The channel fading includes the small scale fading and the large scale fading. The small scale fading is given by the channel model ITU-R M.1225. The channel model A in ITU-R M.1225 has been adopted as the wideband propagation model in the 2GHz band in LEO satellite network, in which the rice factor is 10dB and the maximum Doppler shift is about 35kHz. The large scale fading follows log-normally distribution with mean $\mu = 0dB$ and standard deviation $\sigma = 3dB$ [1], [13]-[14]. In the simulations, the capture effect is also considered for RA system with the large scale fading channel, and the capture threshold is set to 5dB. Furthermore, the original TDMA frame is assumed to be composed of 200 slots and the number of iterations is set

to 16. For simplicity, it is assumed that three different MCSs are considered for APL-assisted CRDSA-like schemes. Three different packet lengths P_1, P_2 and P_3 with durations of T_{P1}, T_{P2} and T_{P3} ($T_{P1} = 2T_{P2} = 4T_{P3}$) are selected to carry a given amount of bit information for the selected MCSs. The main parameters of satellite system with the proposed RA scheme are depicted in Table.1.

TABLE 1. Simulation parameters.

Parameter	Value
Modulation scheme	BPSK, QPSK, 8PSK
Encode type	2/3 3GPP Turbo code
Channel model	ITU-R M.1225
No. of Sub-carrier/IFFT size(N)	512
Message Block Size/DFT size(M)	64
Number of bits in a packet	1280

A. PACKETS WITH DIFFERENT LENGTHS AND THEIR DISTRIBUTIONS

In this subsection, the method to generate packets with different lengths in MBSs in APL-assisted random access system is given, and the distribution of packets with different lengths in the coverage of satellite node is also given.

In MBSs, a mapping table between SNR ranges and MCSs for a given PER is employed in the generation of packets with different lengths. First, the MBSs select their MCSs according to their estimated SNRs from the mapping table, then convert the given bits into complex modulation data with the selected MCSs, and form the packets with preamble and pilots. Different MCSs result in packets with different lengths.

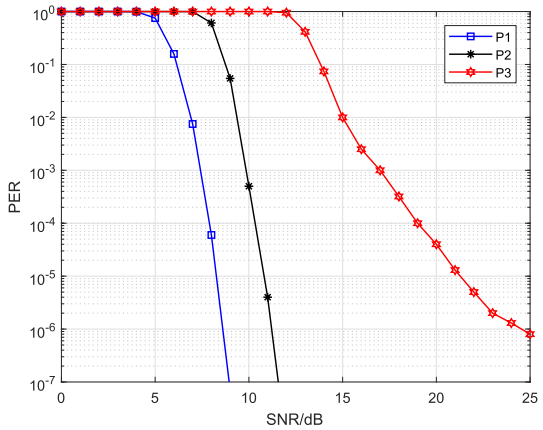

FIGURE 5. SNR vs. PER for different length of packets in APL-assisted schemes.

In the generation of packets, the mapping table between SNR ranges and MCSs for a given PER is very important, which is obtained by PER curves of packets with different lengths. The PERs vs. SNRs curves are obtained by computer simulations in satellite channel. Fig.5 shows the PER performance of packets with three lengths in the IoT oriented LEO satellite network. It can be seen that SNR ranges for three packet lengths P_1, P_2 and P_3 are [6.8dB, 9.5dB], [9.5dB, 15dB] and [15dB, $+\infty$] for the given PER is below 0.01, respectively. The mapping table between MCSs and SNR ranges for three packet lengths is shown in Table.2. In particular, if the SNR is less than 6.8dB, MBS does not send data packets to satellite node since the transmission quality of the channel cannot reach the decoding threshold at this time.

TABLE 2. Mapping table of MCSs and SNR ranges.

Index of MCS (modulation order, encode rate)	Length of packet (SC-IFDMA symbols)	Range of SNR
MCS1: BPSK, 2/3	40	[6.8dB, 9.5dB)
MCS2: QPSK, 2/3	20	[9.5dB, 15dB)
MCS3: 8PSK, 2/3	10	[15dB, $+\infty$]

To investigate the performance of the APL-assisted RA system in all the coverage of satellite node, for the given parameters of RA system, link budget of uplink in the coverage area is conducted, and the distribution of SNRs can be obtained. With the SNRs distributed in the coverage, the distribution of packets with different lengths selected by MBSs can be given in Fig.6. The proportions of packet with lengths of P_1, P_2 and P_3 are 24%, 62% and 14% respectively in the case of uniform distribution of MBSs within the coverage area of LEO satellite node.

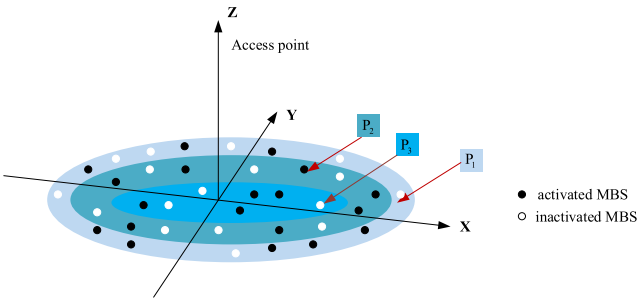

FIGURE 6. Corresponding areas of packets with different lengths.

B. PERFORMANCE OF APL-ASSISTED RA SCHEMES WITHOUT THE CAPTURE EFFECT

To verify the upper and the lower bound of analytical throughput, and the performance of the proposed schemes, computer simulations have been conducted. In the simulations, only the channel model ITU-R M.1225 with small scale fading is considered, and the capture effect is not considered.

The normalized load G is defined as the ratio of the number of data packets arriving in a frame to the slots contained in the frame, as shown in Eq.(19). The normalized load G is measured in packets per slot.

$$G = \frac{\gamma}{M_{slots}^{RA}} \tag{19}$$

where γ is the number of data packets that arrive in a frame, and M_{slots}^{RA} is the number of slots in the frame.

The normalized throughput $T(G)$ under the load G is defined as the ratio of the number of successfully decoded packets in a frame under the load G in the RA system to the number of slots contained in a frame, also measured in packets/slot.

$$T(G) = \frac{\varepsilon(G)}{M_{slots}^{RA}} \tag{20}$$

where $\varepsilon(G)$ the number of successfully decoded packets in a frame under the load G.

The MAC packet loss ratio (PLR) is defined as Eq.(21).

$$PLR = 1 - \frac{T(G)}{G} \tag{21}$$

where G is the normalized load and $T(G)$ is the normalized MAC throughput under the load G.

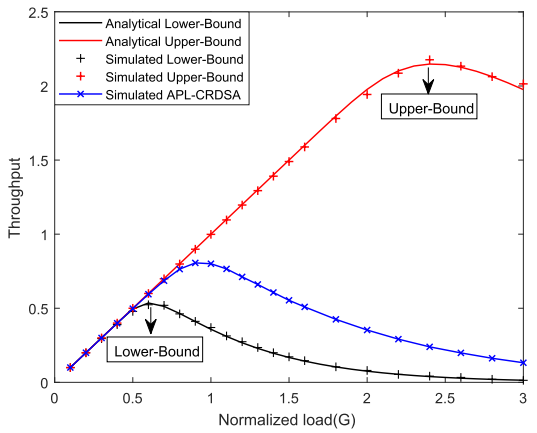

FIGURE 7. Simulated and analytical throughputs vs. normalized load for the APL-CRDSA.

Fig.7 illustrates the Lower-Bound and the Upper-Bound on the throughput of APL-CRDSA. It can be seen that the simulation results are in agreement with the analytical bounds. In addition, the simulated throughput of APL-CRDSA is in the middle of the lower bound and the upper bound, since the proportions of packet lengths P_1, P_2 and P_3 are 24%, 62% and 14% respectively.

Fig.8 shows the throughputs of APL-assisted schemes and their conventional schemes. It can be seen from Fig.8 that the adoption of APL greatly improves the throughput performance compared to the traditional ones. With APL assisted, CRDSA, CRDSA-3 and IRSA achieve their peak throughput about 0.8, 1 and 1.1 respectively. In addition, APL-IRSA achieves linear throughput up to a normalized load of 1, whereas IRSA achieves a similar behavior only up to 0.7.

Fig.9 shows the PLRs of the proposed and conventional schemes. It can be found that APL-CRDSA-3 has the lowest PLR when the channel load is below 1, whereas APL-IRSA achieves the lowest PLR when the channel load is over 1. The results show that the APL-CRDSA-3 and APL-IRSA can be loaded about 2 times those of the CRDSA-3 and IRSA respectively for $PLR = 10^{-3}$.

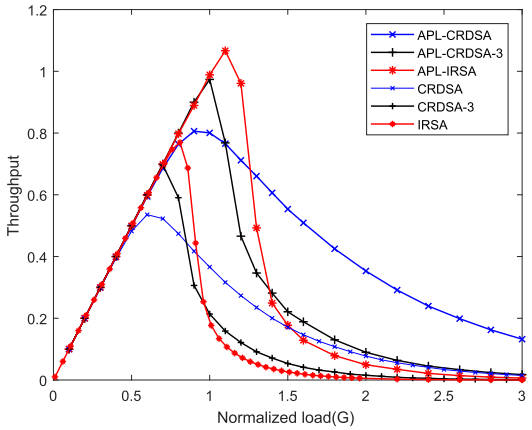

FIGURE 8. Normalized throughputs vs. normalized load.

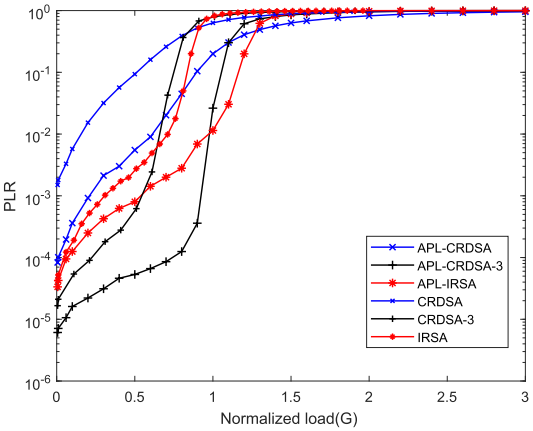

FIGURE 9. Packet loss rate vs. normalized load.

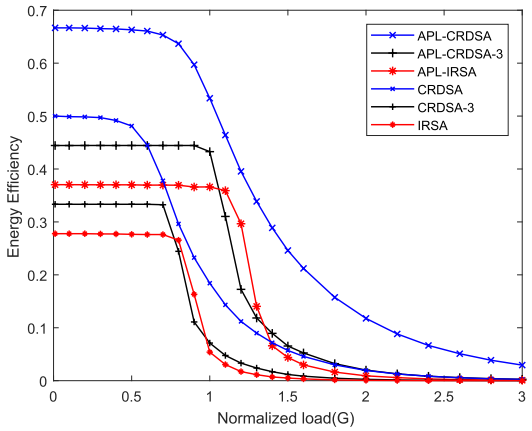

FIGURE 10. Energy efficiency vs. normalized load.

Fig.10 represents the energy efficiencies [6] of the schemes mentioned above. It can be observed that the energy efficiency of APL-CRDSA is higher than 0.65, and CRDSA is only about 0.5 when the normalized load is below 0.8. When the load is below 2, the energy efficiencies of APL-CRDSA-3 and APL-IRSA also yield better performance than those of their conventional ones.

C. PERFORMANCE OF APL-ASSISTED RA SCHEMES WITH THE CAPTURE EFFECT

To show the performance of the proposed schemes in the real environment, the throughput, PLR and energy efficiency are investigated in the channel with the large scale fading. The large scale fading causes the power unbalance of the received signals from different MBSs. The capture effect is considered and the capture threshold is 5dB.

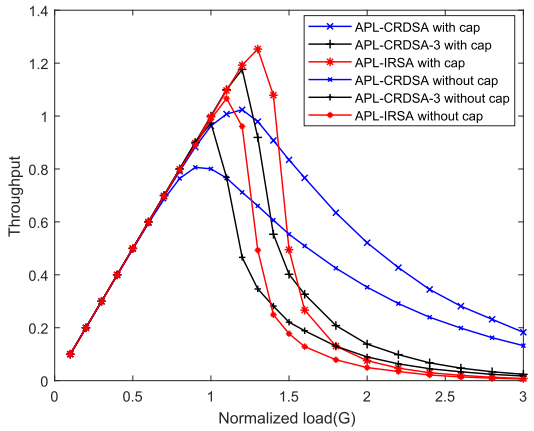

FIGURE 11. Normalized throughputs vs. normalized load.

The throughputs of APL-assisted schemes with and without the capture effect are illustrated in Fig.11. It can be seen from Fig.11 that the APL-assisted schemes with the capture effect outperform those without the capture effect. The superior throughput of APL-CRDSA is obtained about 1 when the normalized MAC load G is 1.2 with the capture effect, resulting in a throughput gain of 20% with respect to that without the capture effect. Furthermore, the throughput of APL-IRSA with the capture effect is greater than 1.2 when the normalized MAC load G is 1.3.

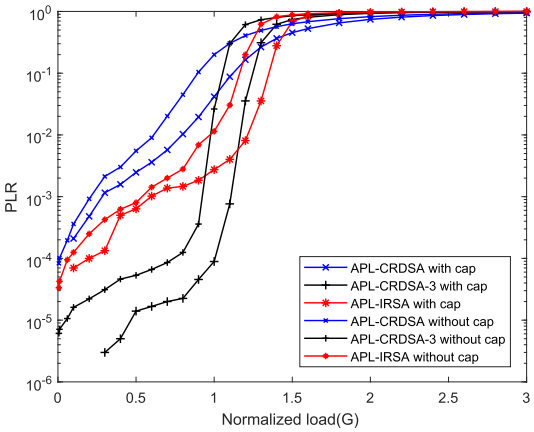

FIGURE 12. Packet loss rate vs. Normalized load.

In Fig.12, the PLRs of the proposed schemes with and without the capture effect are given. As we can see, the capture effect that utilizes the power unbalance gives a positive impact on the PLR performance for all the APL-assisted schemes. With the capture effect, APL-CRDSA-3 has the lowest PLR when the channel load is below 1.2, whereas APL-IRSA achieves the lowest PLR when the channel load is over 1.2. For a target PLR of 10^{-2}, the channel load of APL-CRDSA is 1.2 times as large as that without the capture effect.

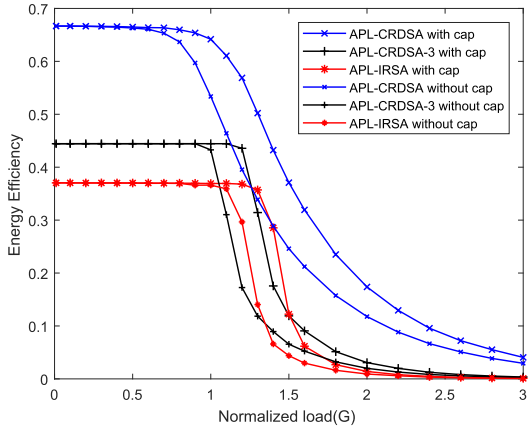

FIGURE 13. Energy efficiency vs. normalized load.

Fig.13 represents the energy efficiency performance of APL-assisted schemes with and without the capture effect. It can be seen that the energy efficiency of APL-CRDSA with the capture effect is greater than that without the capture effect when the normalized load is over 0.9. The APL-CRDSA-3 and APL-IRSA with the capture effect also show better energy efficiency than those without the capture effect, particularly when the normalized load is between 1 and 2.

V. CONCLUSION

In this paper, the adaptive packet-length assisted random access (RA) scheme has been introduced and analyzed. The proposed APL-assisted CRDSA-like schemes exploit the transmission quality in the LEO satellite system and employ the different lengths of packets for different MBSs. Although the decoding process at the gateway introduces some complexity with APL-assisted, the throughput performance, PLR performance and the energy efficiency of RA have been greatly improved compared to those of the conventional CRDSA, CRDSA-3 and IRSA schemes. With the capture effect, the performance of APL-assisted schemes would be further improved and the peak throughput of APL-CRDSA achieves about 1 for the capture threshold of 5dB. Furthermore, the idea of adaptive packet-length assisted gives a novel way to enhance the performance of SA class protocols. The employment of the proposed method can improve the throughput performance of SA class protocols, and meet the need of the large-capacity IoT users accessing the LEO satellite network in the future.

REFERENCES

[1] E. Casini, R. De Gaudenzi, and O. del Rio Herrero, "Contention resolution diversity slotted ALOHA (CRDSA): An enhanced random access scheme-for satellite access packet networks," *IEEE Trans. Wireless Commun.*, vol. 6, no. 4, pp. 1408–1419, Apr. 2007.

[2] R. De Gaudenzi and O. del Rio Herrero, "Advances in random access protocols for satellite networks," in *Proc. Int. Workshop Satell. Space Commun.*, Sep. 2009, pp. 331–336.

[3] G. Liva, "Graph-based analysis and optimization of contention resolution diversity slotted ALOHA," *IEEE Trans. Commun.*, vol. 59, no. 2, pp. 477–487, Feb. 2011.

[4] F. Clazzer, E. Paolini, I. Mambelli, and Č. Stefanović, "Irregular repetition slotted ALOHA over the Rayleigh block fading channel with capture," in *Proc. IEEE Int. Conf. Commun.*, May 2017, pp. 1–6.

[5] E. Paolini, G. Liva, and M. Chiani, "High throughput random access via codes on graphs: Coded slotted ALOHA," in *Proc. IEEE Int. Conf. Commun.*, Jun. 2011, pp. 1–6.

[6] J. Bai and G. Ren, "Polarized MIMO slotted ALOHA random access scheme in satellite network," *IEEE Access*, vol. 5, pp. 26354–26363, 2017.

[7] O. Kodheli, A. Guidotti, and A. Vanelli-Coralli, "Integration of satellites in 5G through LEO constellations," in *Proc. IEEE Global Commun. Conf.*, Singapore, Dec. 2017, pp. 1–6.

[8] G. Cocco and C. Ibars, "On the feasibility of satellite M2M systems," in *Proc. 30th AIAA Int. Commun. Satell. Syst. Conf. (ICSSC)*, Ottawa, ON, Canada, Sep. 2012, p. 15074.

[9] S. Kumar, S. Majhi, and C. Yuen, "Multi-user CFOs estimation for SC-FDMA system over frequency selective fading channels," *IEEE Access*, vol. 6, pp. 43146–43156, 2018.

[10] S. Dimitrov, "Non-linear distortion noise cancellation for satellite return links," in *Proc. IEEE Int. Conf. Commun.(ICC)*, Kuala Lumpur, Malaysia, May 2016, pp. 1–6.

[11] P. T. Mathiopoulos, E. A. Candreva, A. B. Awoseyila, V. Dalakas, D. Tarchi, B. G. Evans, A. Vanelli-Coralli, and G. E. Corazza, "Performance improvement techniques for the DVB–RCS2 return link air interface," *Int. J. Satell. Commun. Netw.*, vol. 33, no. 5, pp. 371–390, 2015.

[12] J. A. Alzubi, O. A. Alzubi, and T. M. Chen, *Forward Error Correction Based on Algebraic-Geometric Theory*. Berlin, Germany: Springer, 2014.

[13] A. Mengali, R. De Gaudenzi, and P.-D. Arapoglou, "Enhancing the physical layer of contention resolution diversity slotted ALOHA," *IEEE Trans. Commun.*, vol. 65, no. 10, pp. 4295–4308, Oct. 2017.

[14] P. Li, Y. He, G. Cui, J. He, and W. Wang, "Asynchronous cooperative Aloha for multi-receiver satellite communication networks," *IEEE Commun. Lett.*, vol. 21, no. 6, pp. 1321–1324, Jun. 2017.

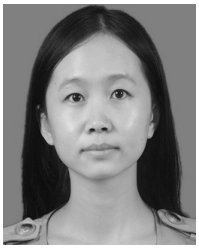

JIALING BAI was born in Shaanxi, China, in 1994. She received the B.S. degree in communications engineering from Xidian University, Xi'an, China, in 2016, where she is currently pursuing the M.S. degree in communication and information systems. Her research interest includes M2M satellite networks.

GUANGLIANG REN (M'06) was born in Jiangsu, China, in 1971. He received the B.S. degree in communications engineering from Xidian University, Xian, China, in 1993, the M.S. degree in signal processing from the Academy of China Ordnance, Beijing, China, in 1996, and the Ph.D. degree in communications and information systems from Xidian University, in 2006, where he is currently a Professor with the School of Telecommunications Engineering. He has authored over 40 research papers in journals and conference proceedings, such as the IEEE TRANSACTIONS ON WIRELESS COMMUNICATIONS, the IEEE TRANSACTIONS ON COMMUNICATIONS, and the IEEE TRANSACTIONS ON VEHICULAR TECHNOLOGY. He has coauthored three books. His research interests include wireless communications and digital signal processing, particularly multiple-input-multiple-output systems, WiMax, and LTE.